

Manipulation of C₆₀ on the Si(001) surface: Experiment and theoryN. Martsinovich,¹ C. Hobbs,¹ L. Kantorovich,¹ R. H. J. Fawcett,² M. J. Humphry,² D. L. Keeling,² and P. H. Beton²¹*Department of Physics, King's College London, Strand, London, WC2R 2LS, United Kingdom*²*School of Physics and Astronomy, University of Nottingham, Nottingham NG7 2RD, United Kingdom*

(Received 28 January 2006; revised manuscript received 17 June 2006; published 3 August 2006)

We extend our previous discussion [D. L. Keeling *et al.*, Phys. Rev. Lett. **94**, 146104 (2005)] of molecular rolling on reactive surfaces. Experimental results showing long-range quasiperiodic tip responses with periods of two, three, and four lattice constants are presented. In addition, we show systematic change of the repeating wave form which we attribute to a slow variation of the tip-sample junction at an atomic level. Using *ab initio* simulations, we have reexamined the translation of C₆₀ across the surface and confirmed our proposed pivoting mechanism via which the molecule rolls by sequential breaking and forming bonds with the surface. A complex character of the molecular displacement, which is accompanied by a substantial deformation of the molecule and the surface, is revealed by careful analysis of the atomic geometry and the electron density redistribution along the path. A large variety of observed tip traces along the trough are then explained by analyzing in detail all possible transition paths between the known stable adsorption sites. Detailed models for the periodic traces with two and three lattice constants are also suggested based on a modified pivoting mechanism. In addition, we predict and discuss possible along-the-row manipulation paths.

DOI: [10.1103/PhysRevB.74.085304](https://doi.org/10.1103/PhysRevB.74.085304)

PACS number(s): 68.43.Bc, 68.37.Ef, 68.43.Jk, 82.37.Gk

I. INTRODUCTION

There is a lot of interest at present in the manipulation of single atoms and molecules adsorbed on crystal surfaces. Controlled manipulation can be potentially used both to seed and/or assemble nanostructures. Scanning tunneling microscopy (STM) has proven to be a successful tool for molecular manipulation.¹⁻³ In particular, manipulation of a C₆₀ molecule on the clean 2×1-reconstructed Si(001) surface has been performed experimentally using STM.^{4,5} Recorded STM tip trajectories show that the movement of the C₆₀ molecule is a complex process that in many cases possesses a long-range periodicity. Periodicities of 3a₀ and 4a₀ were recorded in the manipulation of C₆₀ along the trough (a₀ = 3.84 Å is the surface lattice constant, i.e., the distance between Si-Si dimers along the row). Thus, in the course of manipulation, the molecule goes through a sequence of adsorption configurations before arriving at an equivalent configuration.

It is interesting and important for controlling manipulation to determine atomic-scale details of the manipulation mechanism. Theoretical information on the manipulation of molecules adsorbed on crystal surfaces is rather limited. This is different from the situation with the studies of atomic diffusion and manipulation. Manipulation of single atoms using SPM (scanning probe microscopy) has been modeled theoretically (see Ref. 6 and references therein). There are also many studies on diffusion of adatoms on surfaces (see, e.g., Ref. 7). Manipulation of molecules has been performed experimentally (see Ref. 8 for a review), but theoretical studies of manipulation so far dealt only with small molecules, such as CO on metal surfaces.⁹ We are not aware of theoretical studies of the manipulation of complex organic molecules capable of forming covalent bonds with reactive surfaces.

In our earlier study,⁴ STM images and manipulation trajectories were analyzed in order to identify a mechanism for the movement of the molecule across the surface. One of the

experimental results that shed light on the manipulation mechanism is the observed change in the intramolecular features of C₆₀ in STM images that were taken before and after manipulation events at equivalent adsorption sites.⁵ This points to a change in the adsorption configuration of C₆₀ and implies that the molecule rolls rather than slides on the surface (otherwise, with sliding, the molecule would arrive at the same adsorption configuration after each displacement by a₀). Sliding motion is also unlikely because it would require simultaneous breaking of all bonds between the molecule and the surface and therefore would involve very high energy barriers.

In Ref. 4 we proposed a pivoting mechanism for C₆₀ rolling on the Si(001) surface. The mechanism operates as follows. In stable adsorption configurations, the molecule forms four bonds with the surface. As the molecule is pushed forward by the STM tip during the repulsive manipulation, the two “back” bonds are broken and the two remaining bonds act as a pivot over which the molecule rolls. As the molecule moves further, it forms two new bonds with the surface in addition to the unbroken bonds which act as a pivot, and thus arrives again at a stable adsorption configuration with four Si-C bonds.

This mechanism can only be verified with atomistic calculations. The first *ab initio* simulations of a section of a C₆₀ manipulation pathway along the trough of the Si(001) surface was reported in.⁴ The calculations confirmed the proposed pivoting mechanism for the C₆₀ manipulation.

In this paper we present experimental and theoretical evidence for the C₆₀ rolling during its repulsive manipulation on the Si(001) surface. We report 2a₀ long-range quasiperiodic tip traces for the first time, alongside 3a₀ and 4a₀ traces. In addition, we show quasiperiodic traces in which the strength of subharmonic features varies in a systematic manner. This is attributed to a slow variation of the detailed configuration of the tip-molecule junction.

In order to explain several of the observed tip traces, we

have undertaken an extensive set of *ab initio* calculations to elucidate microscopic mechanisms which can be responsible for the C_{60} translation along the trough. In particular, we suggest detailed mechanisms for the $2a_0$ and $3a_0$ periodic wave forms observed, and also derive other possible transition paths with the $4a_0$ periodicity in addition to the one proposed in Ref. 4. This analysis is based entirely on the pivoting mechanism and our detailed knowledge of all available stable adsorption sites for the C_{60} adsorption on the surface.^{10–12} We extend this approach to predict all possible manipulation pathways for on-the-row manipulation, although these have not yet been reported experimentally.

The paper is organized as follows. In the next section we report our experimental results including the details of the experiments. The results of *ab initio* modeling of a part of a particular manipulation path are presented in Sec. III, where the details of the theoretical method we used is also briefly outlined. Then, in Sec. IV, assuming the pivoting mechanism, we derive more manipulation trajectories from the known stable sites, and discuss their relevance to the tip traces observed experimentally. In particular, we work out all possible pathways along the trough and the row.

II. EXPERIMENT

A. Experimental details

Experiments are performed using a scanning tunneling microscope operating at room temperature under ultrahigh vacuum (UHV) conditions (base pressure 1×10^{-10} Torr). A Si(100)- 2×1 surface is prepared by first loading a $3 \text{ mm} \times 7 \text{ mm}$ piece of a p-type Si wafer and outgassing overnight at 600°C . This is followed by flash annealing the sample at 1200°C for 60 s then further annealing at 800°C for approximately 10 min. C_{60} is sublimed onto the sample at a typical rate of two monolayers per h. Electrochemically etched tungsten tips are used for both imaging and manipulation. The tips are cleaned by electron beam heating prior to use.

STM images are acquired in constant current mode using, typically, a sample voltage of -3 V and a target tunnel current of $0.05\text{--}0.1 \text{ nA}$. The inset to Fig. 1 shows an STM image in which the adsorbed fullerene is resolved as a bright topographic feature with an apparent diameter of $\sim 22 \text{ \AA}$. Also resolved in the background to this image are horizontal bright features which correspond to rows of Si dimers. The molecule is adsorbed with its center in the trough between dimer rows as shown in the schematic in Fig. 1. See Refs. 5 and 13–15 for more details of the Si(100)- 2×1 surface and C_{60} adsorption. Manipulation of C_{60} has been demonstrated both parallel and perpendicular to the Si dimer rows⁵ and in both an attractive and repulsive mode of operation.¹⁶ Here we focus on manipulation parallel to the dimer rows in repulsive mode which, under appropriate conditions leads to a complex tip trajectory which we have recently shown is characteristic of molecular rolling.⁴

Manipulation is induced by first locating a target molecule. The tip is then scanned along a single line which runs parallel to the dimer rows on the Si(100)- 2×1 surface and intersects the center of the molecule. The feedback loop is

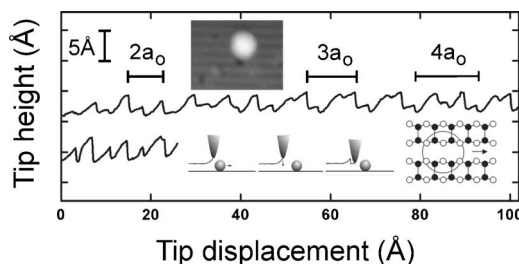


FIG. 1. Linescans acquired during manipulation showing quasi-periodicity equal to two lattice constants. In the upper trace (acquired in constant current mode, sample voltage -1.7 V , tunnel current 1.3 nA) the section from $0\text{--}30 \text{ \AA}$ has a quasiperiodicity equal to $2a_0$. This is followed by a section with a quasiperiodicity equal to $3a_0$ followed by a section with a single wave form of length $4a_0$ which is very similar to that previously observed. The lower trace (constant current mode, voltage -1.6 V , tunnel current 2.0 nA) has a quasiperiodicity equal to $2a_0$. Insets show an image of C_{60} on Si(100)- 2×1 in which the dimer rows may be resolved, a schematic of the repulsive manipulation process which leads to a sawtooth response and a schematic of the adsorption site of C_{60} (large circle) relative to the rows of Si dimers (filled circles)—the arrow indicates the direction of translational manipulation.

active during this linescan and, under standard imaging conditions (-3 V , 0.1 nA), the topographic information acquired during this procedure corresponds to a profile of the molecule.¹⁷ On adjusting the sample bias and target tunnel current to suitable values (typically -1 V , 1 nA) translation of the molecule along a trough bounded by two dimer rows may be induced. Following the approach of Bartels *et al.*² the tip trajectory during manipulation is recorded, and from this data we are able to distinguish between pushing, pulling, and rolling. A typical sawtooth tip trajectory in the *repulsive* mode (pushing) consists of an initial retraction of the tip as it encounters the molecule followed by a sharp extension towards the surface, as the molecule jumps away from the tip, see the schematic in Fig. 1.

B. Experimental results

In this section we consider several experimental traces which extend our recent discussion of molecular rolling. In particular we demonstrate a tip response with a period of two lattice constants in addition to the traces with three and four lattice constants which we have previously reported in Ref. 4. We also consider the issue of reproducibility, particularly in relation to traces characteristic of rolling in which the subharmonic features vary in a systematic manner.

In some traces to be discussed presently the wave forms in a sequence are not exactly identical to each other. In these cases the term “quasiperiodic” may be more appropriate than “periodic.”

Figure 1 shows two tip trajectories acquired during manipulation. In these traces the discontinuous movements of the tip towards the surface are signatures of a repulsive translation of the molecule through one lattice constant.² The quasiperiodic features apparent in Fig. 1 have an overall period equal to integer number of lattice constants, but have a wave

form with subharmonic features separated, approximately, by one lattice constant. The long range periodicity is thus due to successive translational steps through a single lattice constant in which the tip height required to induce manipulation varies in a sequence with longer range periodicity. We have shown⁴ that this is due to a regular sequence of changes in molecular orientation which are coupled to translation displacement.

In the upper trace there are several sections with different periodicities. From left to right (corresponding to the motion of the tip) we observe a section with a periodicity of two lattice constants. This is followed by a section with a periodicity of three lattice constants and a single wave form which is characteristic of the response with a period of four lattice constants. This switching between responses with periodicities with different integer multiples of a lattice constant has been reported previously. However, the observation of a sequence with a periodicity of two lattice constants is new. Another trace with this periodicity is shown in Fig. 1. Each trace has a rather similar wave form confirming that these are examples of a response which recurs and can be initiated with some degree of reproducibility.

Following our previous work we interpret such traces as evidence of a molecular response in which changes in the adsorption state, corresponding to orientation, of C_{60} are coupled to lateral translation of the molecule. In fact there are two possible explanations for the origin of a response with a period of two lattice constants. The first is a rolling mechanism in which molecules pivot over two unbroken bonds. This mechanism is a direct analogy of that previously invoked for the response with a period of four lattice constants, but involving different adsorption configurations. An alternative explanation, discussed in more detail in Sec. IV, is that the molecule undergoes a combination of rolling and rotation around an axis perpendicular to the surface. This is possible if the molecule is connected by one, rather than two, bonds during manipulation, and we argue below that this is a more likely explanation.

We now consider the issue of *reproducibility* for this type of experiment. First we emphasize that there are many aspects, for example the wave form shape, which are highly reproducible and have been observed in our laboratory to recur over experimental runs spanning several years. However, it is also clear that there are several aspects of this type of experiment which are difficult to control. The two major limitations relate firstly to the precision of specifying the initial conditions prior to manipulation, and secondly the exact state of the tip. The initial placement of the tip is achieved by acquiring in a quasicontinuous mode line scans showing topographic profiles perpendicular to the manipulation direction, i.e., across the dimer rows. The quasicontinuous acquisition is necessary to minimize the effects of thermal drift which is ever present at room temperature. We estimate that we achieve a placement accuracy of 0.1 \AA of the initial tip position using this approach. The angle between the tip trajectory and the dimer rows is minimized by rotating the effective scan direction as explained by Humphry *et al.*¹⁷ This is particularly critical since a 1° misalignment in angle over a 100 \AA trace leads to a displacement of the tip of 1.7 \AA towards the dimer row. Thus the

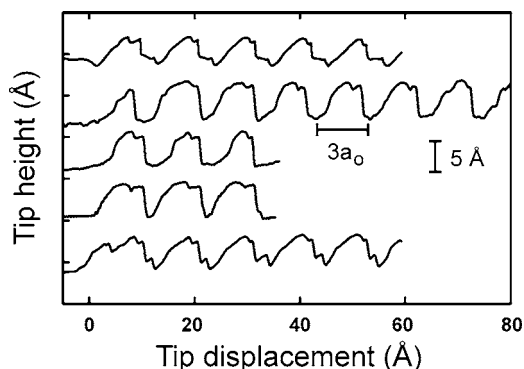


FIG. 2. Several experimentally acquired linescans with a wave form repeating with a period equal to $3a_0$. In the upper trace the relative strength of peaks varies from wave form to wave form indicating that the tip-molecule interaction is varying in a systematic manner from one manipulation event to another—this is attributed to a steady variation in the tip-molecule contact due to misalignment and/or thermal drift. The different wave forms which are observed for different traces (see lower four linescans) are similarly attributed to a variation in initial conditions in tip placement and alignment. The voltage and current used to acquire these traces are (top to bottom): -1.0 V , 1.65 nA ; -1.7 V , 1.2 nA ; -1.6 V , 1.2 nA ; -1.8 V , 1.2 nA ; -1.7 V , 1.2 nA .

“point of contact” between tip and molecule would also vary. While this is naturally a concern it is also worth noting that the response to manipulation for C_{60} on Si(100)- 2×1 may well be rather tolerant to this type of displacement. In our earlier work⁵ we showed that there was a guiding effect of the dimer rows in controlling manipulation and the mechanism which we have proposed for molecular rolling⁴ is closely related to the geometry of the surface atoms and is therefore consistent with this type of guiding.

We have observed several traces which we believe show a variation in the relative tip-molecule position due to either thermal drift, misalignment or their combination. Figure 2 shows an example of such a trace (the upper curve) in which a molecule exhibits a response with a periodicity of three lattice constants. Although the trace and features are rather similar to those published previously the wave form varies in a systematic manner over the trace. In particular, the relative heights of the peaks within the wave form change. These small changes indicate that there is a small, and systematically varying, change in the precise interactions which give rise to manipulation. We attribute the origin of these changes to the tip displacement as described above.

While the upper curve in Fig. 2 shows that the wave form may vary during a single trace, we make the further observation that there are also differences between wave forms of different traces, even where there is no variation of the wave form during the trace. We show more examples of wave forms with a period of three lattice constants in Fig. 2. It is clear that the wave form is slightly different in some traces with some peaks being difficult to pick out at all. Following the argument above we attribute these differences to limitations of the placement and alignment accuracy of the initial tip position.

The details of the atomic configuration will clearly affect the outcome of our experiments. The tips we use are etched

from polycrystalline wire and so there is an intrinsic randomness to the configuration of the tip apex. Furthermore we typically apply voltage pulses of 5–10 V (of either polarity) during imaging to configure the tip into a state in which high quality imaging is possible. This process, and also inadvertent tip crashing which is difficult to avoid at room temperature, can result in uncontrolled transfer of material between the tip and the silicon substrate. We consider it likely that our tip has adsorbed Si atoms at its apex.

Despite this lack of control it is possible, when adopting the procedures described above, to initiate manipulation with the same characteristic features. In this and previous papers we focus only on behavior that is reproducible in the sense that similar traces have been observed many times. Furthermore we stress that periodic traces are intrinsically reproducible since the same behavior, and therefore the same tip-molecule interaction, occurs repeatedly within a given sequence. Nevertheless there are still many attempts at manipulation which do not result in the type of trace discussed in this paper. Alternative outcomes include transfer of a molecule to the tip, some other change to the tip, sometimes catastrophic, or displacement of the molecule in a series of steps in which an extended periodic response cannot be discerned. Overall approximately 10% of the attempts at manipulation result in traces with long-range periodicity. Of these approximately 50% have a period of three lattice constants, 40% have a periodicity of four lattice constants, and 10% have a period of two lattice constants. We attribute these variations in the outcome of attempts at manipulation to variations in the tip configuration (which for room temperature operation is difficult to control) rather than intrinsic randomness in the manipulation process itself.

III. THEORY

A. Theoretical method

We use SIESTA (Ref. 18), a density functional code in the generalized gradient approximation (GGA), with Perdew-Burke-Ernzerhof (PBE) functional¹⁹ for exchange correlation, with norm-conserving pseudopotentials and periodic boundary conditions. A localized double-zeta polarized (DZP) basis set is used to describe the valence electrons, which is composed of a double (split valence) basis for each valence orbital plus polarization functions for all the atoms. The mesh cutoff (which indicates the equivalent plane wave cutoff) used was 150 Ry. The energy shift (i.e., the energy raise suffered by the orbital when confined) was taken as 0.14 eV. This choice of basis results in 13 orbitals for both carbon and silicon with a maximum orbital radius of 5.5 and 6.9 Bohr for the respective elements.

A 188-atom cell was used which contained 60 C atoms, 96 Si atoms (six layers), and 32 terminating H atoms. A vacuum gap of 13 Å was present between the top of the C₆₀ and the bottom of the image silicon slab. The coordinates of the two lowermost layers of Si atoms and all H atoms were fixed. The remaining atoms were allowed to relax until forces on atoms were smaller than 0.04 eV/Å. Only a single **k** point was used in the calculations due to the large size of the simulation cell.

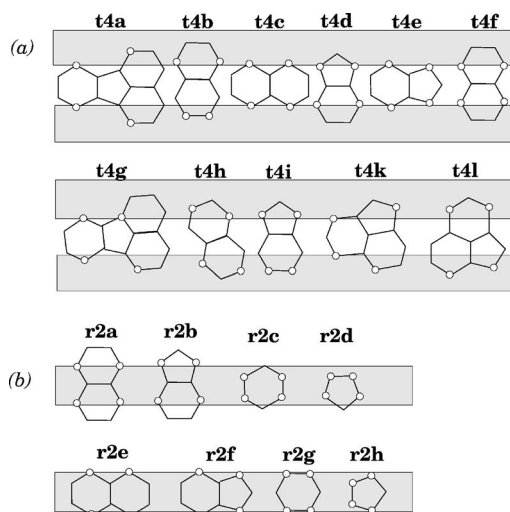


FIG. 3. Schematic pictures of C₆₀ adsorption sites on Si(001): (a) *t4* sites above the trough; (b) *r2* sites above the row.

A well-known problem associated with the use of localized basis sets applied to compound systems is the basis set superposition error (BSSE). In our calculations the BSSE correction is accounted for according to the Boys-Bernardi counterpoise method²⁰ as described in Ref. 12.

Electron density difference plots $\Delta\rho(\mathbf{r})$ for the “C₆₀+Si(001)” system were found to be extremely useful in analyzing the detailed changes in chemical bonding in the system along the whole manipulation path. The density difference was constructed by subtracting the densities $\rho_{C_{60}}(\mathbf{r})$ and $\rho_{Si}(\mathbf{r})$ of the isolated C₆₀ and the Si(001) surface from that of the combined system:

$$\Delta\rho(\mathbf{r}) = \rho_{C_{60}+Si}(\mathbf{r}) - \rho_{C_{60}}(\mathbf{r}) - \rho_{Si}(\mathbf{r}). \quad (1)$$

Note that the isolated C₆₀ and the surface are considered at each point along the path in the geometry of the combined system to eliminate spurious density changes due to atomic displacements.

B. *Ab initio* calculations of C₆₀ manipulation

The earlier calculations from our group^{11,12} together with the calculations of Godwin *et al.*¹⁰ identified a large number of stable adsorption configurations for a C₆₀ molecule on the clean Si(001) surface. Stable sites are found to exist above the trough between four dimers and above the row between two dimers, see Fig. 3. They can be characterized by the number of Si-C bonds formed between the molecule and the surface. Stable configurations have three or four bonds, with binding energies typically between –1.6 and –2.8 eV (or 0.4–0.7 eV per Si-C bond), calculated relative to the isolated C₆₀ molecule and the Si(001) surface in the buckled $p(2 \times 1)$ reconstruction.

We use the same notation for adsorption configurations as in Ref. 12: the first letter is either “*t*” (trough) or “*r*” (row), followed by a number (1, 2 or 4) that denotes the number of Si-Si dimers bonded to the C₆₀ molecule, and a letter to label a particular structure.

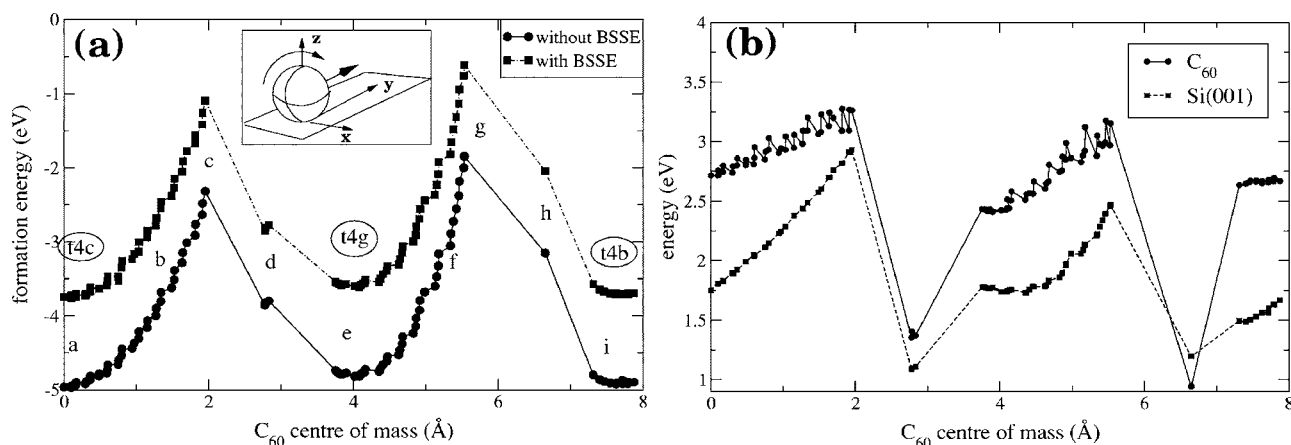


FIG. 4. (a) Binding energies of C_{60} along the manipulation path calculated relative to the *symmetrical* $p(2 \times 1)$ reconstructed Si(001) surface. Stable adsorption configurations $t4c$, $t4g$, and $t4b$ are marked. Inset: a schematic of the C_{60} rolling. (b) Individual energies of C_{60} and the Si(001) surface calculated for the geometries optimized for the C_{60} -surface combined system, shown relative to the corresponding energies of the isolated systems. Labels (a)–(i) correspond to the configurations in Fig. 6.

Configurations $t4a$ – $t4i$ were reported earlier in Refs. 10–12, however, additional sites $t4k$ and $t4l$ were found here. The latter two configurations were identified during our investigation of possible C_{60} manipulation pathways; this is described in more detail in Sec. IV. Both configurations have four Si-C bonds to the surface but relatively low binding energies, -0.68 eV ($t4k$) and -1.07 eV ($t4l$). These can be explained by a significant rebonding within the lower part of the C_{60} molecule. Configurations $r2a$ – $r2g$ above the row were also reported in Refs. 10–12, whereas configuration $r2h$, which has a low binding energy of -0.63 eV and contains a pentagon of the C_{60} facing the silicon surface, is reported here.

Sites above the trough between two opposite dimers or above the row on top of a single dimer were found to be metastable forming two strong Si-C bonds and in certain cases up to two additional weaker bonds. These sites are important, as they may be intermediate states during C_{60} manipulation on the Si(001) surface.

We modeled a part of the tip-induced manipulation path for C_{60} along the trough using density functional theory calculations, as described in Sec. III A. The outline of the main results of these calculations can be found in Ref. 4. Only a $2a_0$ -long part of the manipulation pathway was modeled due to the significant cost of such calculations. A constrained minimization technique was used to model the C_{60} manipulation. For this, a single carbon atom of the C_{60} molecule was chosen and displaced in small steps of 0.05 Å along the trough running in the y direction [see the inset in Fig. 4(a)]. For comparison, in experiment the STM tip was moved in steps of 0.14 Å (Ref. 4). The positions of all other atoms were optimized at each step, and the position of the displaced atom was optimized in the plane perpendicular to the displacement direction.

In spite of the fact that the STM tip is absent in our calculations, we believe that our work is relevant to the investigation of C_{60} manipulation. This is because the displaced atom can be used to model the actual contact of the molecule with the tip that drives the manipulation process. In

particular, pushing may be simulated by an inward displacement of an atom at the rear of the molecule in the direction of the manipulation, while the pulling mechanism—similarly by using one of the front atoms displaced outwards in the same direction, the way it was done in our calculations.

We also think that the tunneling current in STM between the surface and the tip is not the factor responsible for manipulation; its role is mainly to control the tip position. Instead, the role of the tip is to push the molecule. Therefore, our computational approach, where the movement of the C_{60} is conducted by displacing one of its atoms is a valid model to describe externally driven movement of the molecule, as in real STM or atomic force microscopy (AFM) manipulation experiments.

Structure $t4c$, the lowest-energy structure of C_{60} adsorbed on the Si(001) surface, was taken as the starting structure for the simulation. When calculating the binding energies along the manipulation path, the *symmetrical* $p(2 \times 1)$ structure of the Si(001) surface was adopted as a reference since the STM manipulation experiments⁴ were conducted at room temperature. This point requires some explanation. It is well known^{21,22} that above 200 K (the critical temperature, T_c , of the order-disorder phase transition) dimers of the Si(001) surface perform fast flip-flop motion. The cross section of the surface potential energy along the flipping coordinate of any dimer looks like a double well.²³ Since there are many dimers, the potential energy of the surface must be very complicated with two global minima [corresponding to the two possible orientations of the $c(4 \times 2)$ reconstruction] and many local minima and saddle points (corresponding to other configurations of the system when dimers take on all possible orientations). At T_c the total energy of the surface (including the vibrational contribution which is mainly due to oscillating dimers) may be simulated by the highest (saddle) point on the potential energy surface when all dimers take on the symmetrical orientation. This point can be conveniently considered as the surface potential energy above the T_c . At room temperature the surface energy is even higher due to atomic vibrations. However, as we neglect the vibrational

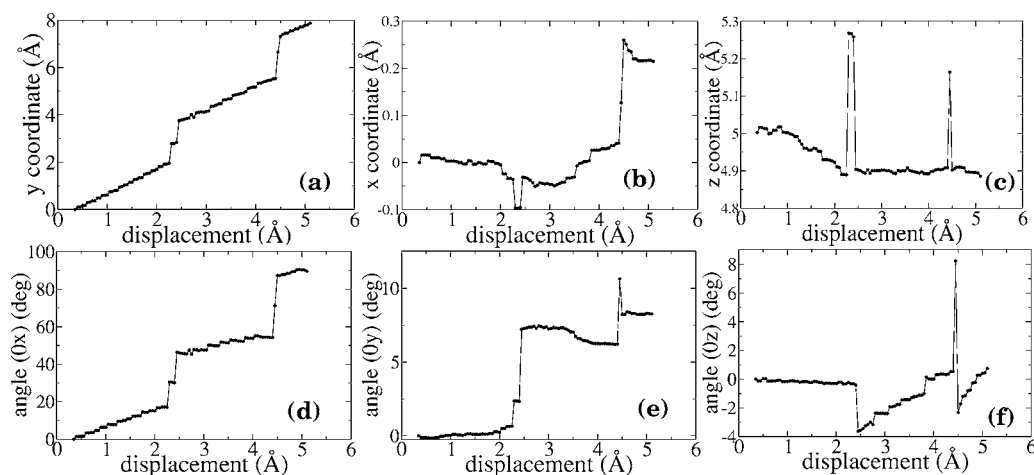


FIG. 5. The trajectory of the C_{60} movement: (a)–(c) y , x , and z coordinates of the molecule’s center of mass during manipulation as a function of displacement of the fixed C atom along the y axis [see inset in Fig. 4(a)]; (d)–(e) angles of rotation of the molecule around the x , y , and z axes (in degrees).

contribution for the combined (C_{60} and the surface) system, it is reasonable to take the surface with symmetrical dimers as a reference to describe the experimental room-temperature C_{60} manipulation. Intuitively this can be easily understood: due to fast flip-flop motion the surface on average can be treated as being in the *symmetrical* $p(2 \times 1)$ phase. Note that in Ref. 4, the buckled $p(2 \times 1)$ reconstruction was used as the reference for the Si(001) surface. Thus, the calculated values of binding energies are somewhat different in that paper.

Figure 4(a) shows the energy of the molecule, relative to the isolated C_{60} and the Si(001) surface, along the manipulation pathway with respect to the position of the C_{60} center of mass. Our simulations give the transition between the configurations $t4c \rightarrow t4g \rightarrow t4b$ (energy minima on the plot), with the energy barriers between them corresponding to transition states. It can be seen in Fig. 4(a) that the energies at first rise until the barrier of 2.5–3 eV is reached. After that there is a fast drop to the next stable configuration. Note that the displacement of the constrained atom was kept constant throughout the simulation. However, the position of the center of mass of the molecule changed by a large amount, as the molecule fell into the next stable configuration. These few steps were also accompanied by a large energy change.

Figure 5 shows the trajectory of the molecule in detail. The x , y , and z coordinates of the center of mass of the molecule are plotted with respect to the displacement of the fixed carbon atom. Recall that the molecule moves along the y direction, as shown schematically in Fig. 4(a). It can be seen from the graphs that there are intervals where the y coordinate of the molecule changes by a large amount during a few displacement steps, whereas most of the time the molecule’s movement proceeds slowly. It can be seen that the molecule advances by ~ 8 Å, or approximately $2a_0$, as it goes through the three configurations. The z coordinate of the molecule (its height above the surface) remains approximately constant along the manipulation path, except for two points—the pivoting steps where the molecule stands on two Si-C bonds rather than on four bonds (the bonding configurations can be seen in Fig. 6). The x coordinate of the mol-

ecule’s center of mass changes slightly along the manipulation path: the molecule wobbles slightly to the sides as it moves. This can also be seen from the angles of rotation of the molecule around the y and z axes: the molecule does not move entirely along a straight line but tilts slightly to one side. The angle of rotation around the x axis, i.e., in the direction of motion, shows that the molecule turned by 90° during displacement by $2a_0$, a quarter of the full turn of the molecule.

It is also worth noting that the second stable configuration, $t4g$, is asymmetric, despite the initial $t4c$ configuration being symmetric. The two possible alternative configurations, $t4a$ and $t4e$, are symmetric but are higher in energy than $t4g$. This fact is due to geometric commensurability of the C_{60} molecule and the Si(001) surface and demonstrates that preserving the symmetry of adsorption configurations is not a necessary requirement in C_{60} manipulation.

In each elementary translation of the molecule by a_0 to the next stable configuration, as we shall show presently, three steps can be identified. At the first step, between the initial stable configuration and the barrier [points (a)–(c) or (e)–(g) in Fig. 4(a) for the first or the second elementary translations, respectively], four C-Si bonds are preserved, but both the molecule and the surface undergo strong deformation. At the second step [points (c)–(d) or (g)–(h)] the two back Si-C bonds are broken, and the molecule has only two bonds to the Si-Si surface dimers. The configurations (d) and (h) belong to the $t2$ group.¹² Thus, the initial $t4c$ configuration is followed by $t2d$ (point d), which is 0.9 eV higher than $t4c$ —close to the value of 1.0 eV found in our earlier static calculations.¹² The next $t2$ -type configuration that follows $t4g$ (point h), although not identified in Ref. 12, has a similar but somewhat higher energy, 1.8 eV higher than $t4c$. Finally, at the last step [points (d)–(e) and (h)–(i)], a new pair of front Si-C bonds is formed, and the molecule moves into a stable adsorption configuration¹² with four C-Si bonds with the surface dimers.

Interestingly, the highest-energy configurations [points (c), (g) in Fig. 4(a)] are not those with two bonds between the molecule and the surface but the configurations where all

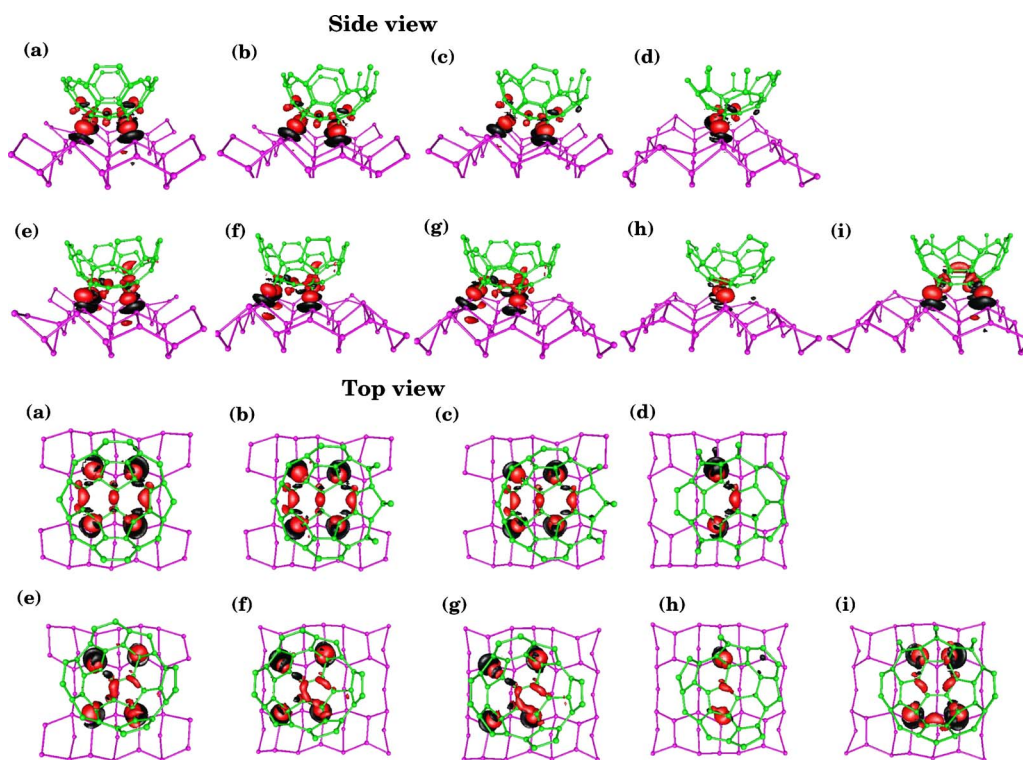


FIG. 6. (Color online) Electron density differences ($\pm 0.035e$) along the manipulation path between the combined C_{60} -silicon system and the isolated C_{60} and silicon surface: top and side views. Regions of the excess and lack of the electron density relative to the isolated C_{60} and silicon are shown in red (dark gray) and black, respectively. Only Si and C atoms close to the bonding interface are shown.

four Si-C bonds are still retained. As we shall argue in Sec. III C, the energy barriers in our calculations are overestimated. Still, we believe, the physical processes during each elementary translation, as summarized above, do still take place.

The path between stable configurations with four Si-C bonds via intermediate configurations having two Si-C bonds is confirmed by electron density difference plots obtained using Eq. (1). These were calculated at a number of points along the path and are shown in Fig. 6. Regions of the excess electron density relative to the isolated C_{60} and silicon are shown in red (dark gray), and those with the lack of it in black.

The Si-C bond formation between the molecule and the surface and changes in the electron density distribution within the C_{60} cage can be seen in the plots. The plots clearly show that the highest-energy points are not the structures with two Si-C bonds but the preceding stages just before the back bonds are broken. Structures with only two Si-C bonds have intermediate energies and are immediately followed by stable structures with four Si-C bonds. An explanation for these energies can also be given based on electron density distribution.

A significant *rebonding* in the C_{60} cage along the manipulation path can be seen in the top views of the molecule in Fig. 6. At the highest points [(c) and (g)] along the path, the electron density distribution in the lower part of the molecule differs strongly from that in isolated C_{60} , and the C-Si bonds are strongly stretched. At these points the system loses a lot of energy. Notably, intermediate structures with two Si-C

bonds [points (d) and (h)] have an electron density distribution rather similar to the isolated molecule. This can balance the effect of breaking two Si-C bonds with the surface and may explain the fact that the highest-energy structures in our calculations are not those with only two Si-C bonds but the immediately preceding ones.

We can semiquantitatively estimate the effect of deformation of the C_{60} -silicon system by considering separately the deformation of the surface, the C_{60} molecule, and the Si-C bonds. Examination of bond lengths and of the geometry of the surface and the C_{60} molecule confirms that the surface atoms are displaced from their stable positions and the molecule is very strongly deformed from its original spherical shape at the highest-energy points.

Figure 4(b) shows the energies of the silicon surface and the C_{60} molecule calculated separately in their geometries optimized for the C_{60} -surface combined system at each point along the manipulation path relative to the energies of the isolated silicon surface and C_{60} . The figure shows that, first, both the molecule and the silicon surface are 1.0–3.5 eV higher in energy along the whole manipulation path than the isolated C_{60} and silicon surface; second, the energies of the C_{60} and silicon increase between points (a)–(c) and (e)–(g) by 0.5–1.0 eV. This means that, as the molecule moves towards the potential energy barrier, both the molecule and the surface become significantly deformed. Finally, points (d) and (h) (the pivoting stages where only two bonds exist between the C_{60} and the surface) are those where the C_{60} and the silicon surface have the lowest energies and are the least distorted compared to optimized isolated geometries.

The response of the C_{60} and other fullerenes to uniaxial and axial deformation was studied theoretically previously.^{24,25} These studies showed that the C_{60} molecule is not a rigid body and that it can withstand strong deformation before a permanent change of shape or collapse of the molecule. The strain energy corresponding to an axial strain of $\sim 4\%$ (similar to the values obtained in our C_{60} manipulation simulations) was of the order of 0.5–0.6 eV.

The Si-C bond lengths have also been analyzed during the manipulation. We find that the front pair of Si-C bonds is normally ~ 2.0 Å long (cf. 1.88 Å the calculated Si-C bond length in bulk cubic silicon carbide), and the back Si-C bonds become 2.30 Å [during the first elementary translation step at point (c) in Fig. 4(a)] or 2.23 Å [during the second step, point (g)] before breaking. The energy change due to the elongation of Si-C bonds can be estimated by varying the lattice parameter of bulk silicon carbide. Based on the c -SiC data, elongation of Si-C bonds from 2.0 to 2.3 Å would cost 0.61 eV per bond, and from 2.0 to 2.23 Å would cost 0.47 eV per bond. This can be compared with the energy effect of Si-C bond formation upon adsorption of C_{60} on the Si(001) surface, 0.4–0.7 eV.¹²

Thus, the combined effect of deformation of the silicon surface and the C_{60} molecule and strained Si-C bonds during the manipulation of the molecule strongly increases the energy of the C_{60} -silicon system. This deformation can be relieved by Si-C bond breaking and subsequent relaxation of the geometry of the C_{60} and the silicon surface and C_{60} rebonding. This process is accompanied by energy lowering. The structures with only two Si-C bonds between the molecule and the surface are metastable, and a small displacement of the molecule can cause the pivoting of the molecule over the remaining two Si-C bonds so that two new Si-C bonds are formed, releasing ~ 1 eV of energy and resulting in a new stable adsorption configuration.

Note that the above calculations may also be relevant for describing self-diffusion of the C_{60} molecule on the same surface, although details may be different. Indeed, it seems highly probable that the mechanism of self-diffusion is rolling as this would require only two bonds with the surface to be broken, rather than four in the sliding mechanism. The issue of C_{60} self-diffusion is interesting in its own right. There have not been systematic studies of C_{60} diffusion on the silicon surface; however, surface diffusion of C_{60} and higher fullerenes was inferred from fullerene desorption data at high temperatures of 300–500° in an experimental study,²⁶ and jumps of the C_{60} from trough to row positions were observed by STM during annealing at 500° (Ref. 15). The experimental results suggest that the barrier to C_{60} diffusion is very high. Hence, we can only give an upper estimate of 2–2.5 eV for the barrier of C_{60} diffusion on the silicon surface from our calculations. Such a high barrier would not allow the diffusion of C_{60} even at room temperature. A displacement of C_{60} has to be driven externally, for example, by means of an STM tip.

C. BSSE corrections

Formation energies described so far and reported in Ref. 4 did not include BSSE corrections as discussed in Sec. III A.

Here we present more careful calculations in which the BSSE correction was estimated at each point along the manipulation pathway. The BSSE values are between 1.17 and 1.26 eV for most of the manipulation path when there are four Si-C bonds, and between 1.0–1.1 eV for configurations with two Si-C bonds. This proves that there is a relatively smaller mutual effect of C_{60} and the silicon surface when only two Si-C bonds exist—the fact already shown by the electron density distribution of the C_{60} -silicon system being similar to that of the isolated C_{60} and silicon surface. We also conclude that the BSSE correction affects the energy barriers very little along the path.

Recall that in these calculations we modeled the C_{60} manipulation at room temperature. To this end, the symmetrical $p(2\times 1)$ Si(001) surface was considered as a reference in calculating the binding energies along the manipulation path. It is seen from Fig. 4(a) that at room temperature the molecule is bound to the surface along the whole transition path.

The situation may be different for low temperatures where the $c(4\times 2)$ reconstruction with buckled dimers is known^{21,22} to be more energetically favorable. In this case, if the $c(4\times 2)$ structure is considered as a reference, the BSSE corrected binding energies near the barrier for the C_{60} manipulation become positive. Note that as the binding energy is defined with respect to the isolated molecule and the surface, the energy cannot be larger than zero since zero binding energy corresponds to the infinite separation of the two. Therefore, obtained positive binding energies are an artifact of our calculation method based on the constrained minimization technique and thus the calculated barriers are overestimated. Even so, the barriers are too large for the molecule to overcome at sufficiently low temperatures, so that this error does not affect our conclusions.

Note that an accurate calculation of the transition path [using, e.g., the nudged elastic band (NEB) method^{27,28}] would be very time consuming taking into account the large size of the system. Still, to estimate the barriers better, one may try a number of methods. One of them is to model C_{60} manipulation in a different way, including the STM tip in the model. These calculations are currently under way. The other approach is to move the molecule by displacing some other atom of the C_{60} molecule. We tried several alternative choices of the carbon atoms to drive the C_{60} manipulation, and find that the energy barriers can be reduced by at least ~ 0.4 eV.

IV. MANIPULATION PATHWAYS

Experiments on the STM manipulation of C_{60} described in Sec. II A provided a rich variety of manipulation trajectories along the trough, including periodic tip traces with periodicities ranging between two and four dimer-dimer distances a_0 . It is not practical to perform extensive *ab initio* modeling of all possible pathways to explain the observed trajectories, since *ab initio* simulations of C_{60} manipulation are very time consuming. However, it is possible to predict manipulation sequences *analytically* by analyzing stable adsorption configurations of C_{60} on Si(001) and possible transitions between them.

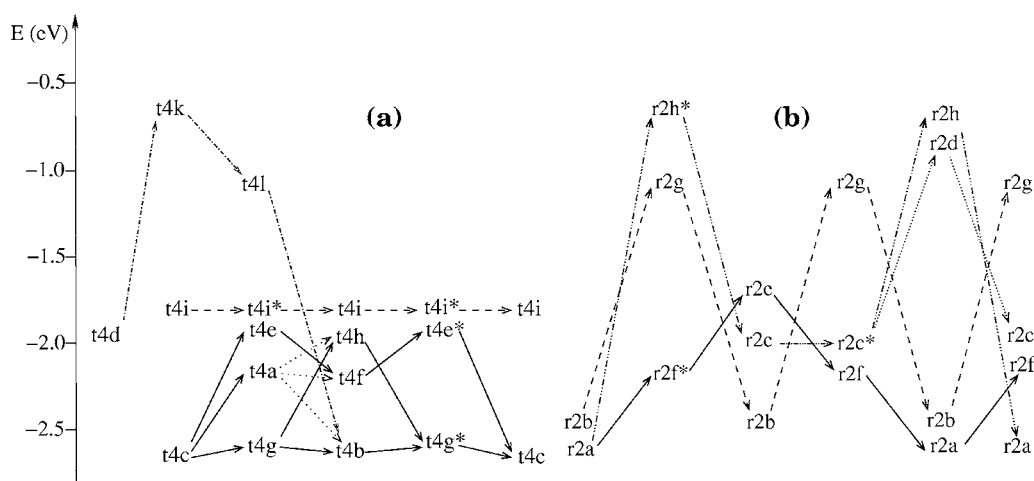


FIG. 7. Possible pathways for C₆₀ rolling along the trough (a) and the row (b). The binding energies correspond to the zero temperature. Solid, dashed, and dotted lines refer to different rolling pathways.

The basic assumptions made when predicting possible manipulation pathways are as follows: (i) the molecule moves between known stable adsorption configurations (with four Si-C bonds) via unstable or metastable transition states having two bonds; (ii) sequential breaking of Si-C bonds and formation of new bonds takes place, i.e., the movement of the molecule occurs via the pivoting mechanism over two front Si-C bonds as first suggested in Ref. 4.

It can be shown, for example, that the pathway described in the previous section and in Ref. 4 is a part of a longer sequence with a $4a_0$ periodicity. An inspection of the bonding in the $t4b$ configuration (the very last one obtained in our *ab initio* calculations of manipulation) and all other adsorption configurations above the trough¹² shows that this configuration can only be followed by the $t4g^*$ configuration (the mirror image of the $t4g$ configuration). Similarly, of all possible configurations, $t4g^*$ can only be followed by $t4c$, i.e., the same configuration as the starting one. Thus, after having gone through four different adsorption configurations, the molecule arrives at the starting configuration. The complete sequence $t4c \rightarrow t4g \rightarrow t4b \rightarrow t4g^* \rightarrow t4c \dots$ therefore has a fourfold periodicity. Note that during each translation from one stable configuration to another the molecule advances by a_0 . Therefore, this manipulation sequence has a periodicity of $4a_0$, the same as observed in our experiments (see also Ref. 4).

Other pathways along the trough may also be possible, starting from or going through different stable configurations. We analyzed all known adsorption configurations in the trough and the possibilities of transitions between them. The possible transitions between pairs of configurations can be summarized as follows: $t4a \rightarrow t4b$, $t4f$ or $t4h$; $t4b \rightarrow t4g^*$; $t4c \rightarrow t4a$, $t4e$ or $t4g$; $t4e \rightarrow t4f$; $t4e^* \rightarrow t4c$; $t4f \rightarrow t4e^*$; $t4g \rightarrow t4b$ or $t4h$; $t4g^* \rightarrow t4c$; $t4h \rightarrow t4e^*$; $t4i \rightarrow t4i^*$. The asterisk here designates the sites which are mirror images of the main sites as described in Ref. 12. By connecting all adsorption sites with arrows corresponding to transitions between them, all possible manipulation pathways can be constructed and these are shown in Fig. 7(a).

It can be seen that the configuration $t4c$, the starting con-

figuration in our *ab initio* simulations, can give rise to several different manipulation sequences: it may arrive upon pivoting not only at site $t4g$ as described above and found in our *ab initio* calculations, but also at some other stable sites: $t4a$ and $t4e$. The configuration $t4g$ may be followed either by $t4b$ (as in our calculations), or by configuration $t4h$, which is higher in energy (has a lower binding energy), and in turn can be followed only by $t4g^*$. This results in a $4a_0$ -periodic sequence that is similar to the one described in the previous section. The configuration $t4e$ can only roll into $t4f$, followed by $t4e^*$, the mirror image of the configuration $t4e$, and finally $t4c$ that is the starting configuration of the sequence. The configuration $t4a$ appears to be a special case: upon pivoting it should arrive at a configuration which is not stable according to our calculations. It can then relax into one of the configurations $t4b$, $t4f$ or $t4h$ upon rebonding with the surface dimers. Therefore, the particular transition from $t4a$ does not exactly correspond to the pivoting mechanism. The configuration $t4i$ can only be followed by its mirror image $t4i^*$ and does not transform into any of the sequences discussed above. Hence, a $2a_0$ periodic sequence can be constructed from these configurations: $t4i \rightarrow t4i^* \rightarrow t4i \rightarrow \dots$. Finally, the site $t4d$ does not take part in any periodic sequences. However, as shown in Fig. 7, the molecule can arrive from configuration $t4d$ to $t4b$ via $t4k$ and $t4l$ shown in Fig. 3(a). Note that the site $t4b$ belongs to the periodic sequence mentioned above.

Thus, if one follows the indicated transitions between stable sites, several sequences can be identified as shown schematically in Fig. 7(a). All the sequences starting at $t4c$ have the $4a_0$ periodicity. There is only one sequence with the $2a_0$ periodicity starting from configuration $t4i$, which is higher in energy than the above-mentioned $4a_0$ periodic sequences.

All the sequences with the $4a_0$ periodicity start from the configuration $t4c$, i.e., the one with the largest binding energy. According to Fig. 7(a), manipulation can, in principle, go along several routes, starting from this configuration, with different energy profiles for different sequences. However, our *ab initio* simulations as described in Ref. 4 and in this

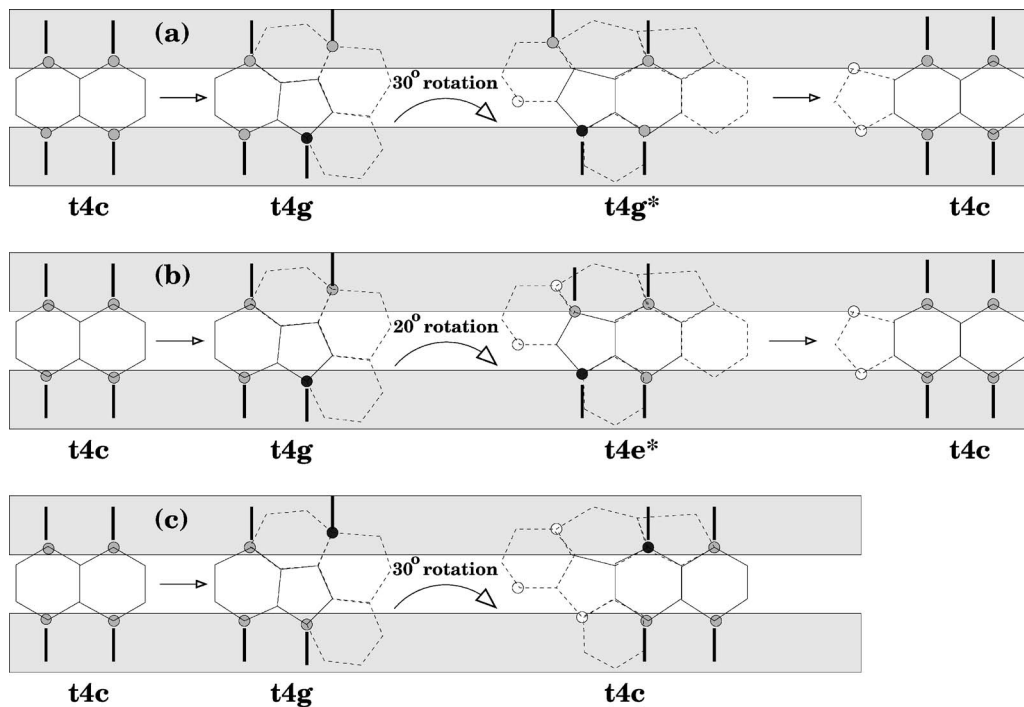


FIG. 8. A schematic of possible mechanisms of C_{60} rolling along the trough with the periodicity of $3a_0$ (a), (b) and $2a_0$ (c). Only lower hexagons and pentagons of the C_{60} are shown. Silicon dimer rows are shown as gray stripes. Shaded circles denote carbon atoms forming Si-C bonds; among them, dark shaded atoms are those which are involved in pivoting over one bond. Empty circles indicate the positions of the Si-C bonds in the preceding configurations and are included to show more clearly the transitions from a previous configuration to the next one. Positions of the Si-Si dimers close to the C_{60} molecule are shown as dark lines.

work give only one path, the one with the lowest energy. It is possible that not all of the conceivable sequences occur in manipulation experiments but only those with the lowest energy. However, various manipulation pathways with the same $4a_0$ periodicity, which are observed in our STM experiments, suggest that, depending on the particular experimental conditions, several sequences in Fig. 7(a) could in principle be involved, not only the one with the lowest energy.

Note that STM manipulation experiments along the trough have recorded $2a_0$, $3a_0$, and $4a_0$ periodicities for the manipulation trajectories, with changes from $4a_0$ to $3a_0$ observed within the same trajectory.⁴ Above, we have proposed a $2a_0$ and several $4a_0$ periodic sequences, among them the lowest-energy path ($t4c \rightarrow t4g \rightarrow t4b \rightarrow t4g^* \rightarrow t4c \dots$), these can explain some of the experimentally observed tip trajectories. However, no $3a_0$ periodic sequence can be identified, based on our assumption of pivoting over two bonds as described above.

An inspection of experimental tip trajectories (see also Ref. 4) with different periodicities shows that there is a close similarity between wave forms of $3a_0$ and $4a_0$ periodic sequences, and a return to the $4a_0$ periodicity can occur after a $3a_0$ sequence. This allows us to conclude that there is a part of the manipulation sequence that is common for manipulation pathways with both periodicities, and a switch from a $4a_0$ to a $3a_0$ sequence occurs at one of the pivoting stages. At this point the mechanism of C_{60} rolling is somewhat altered, for example, by the molecule pivoting over a single bond only. We propose that when the molecule is close to pivoting and has only two bonds to the surface (i.e., is much less

stable), a certain amount of asymmetry in the position of the STM tip can give the molecule a rotational moment about an axis perpendicular to the surface. In this case, the trajectory of the molecule can deviate from the sequences suggested above.

Assuming that only a single bond is retained at the pivoting stage, it is possible to find all possible pathways between the stable sites for this mechanism as well. There is a significant number of possibilities, so that we shall focus only on those that arise from the most energetically favorable transition path $t4c \rightarrow t4g \rightarrow t4b \rightarrow t4g^* \rightarrow t4c \dots$. Among all the stable sites there, the $t4g$ configuration is the one that is likely to give rise to alternative manipulation pathways. For example, by means of bypassing configuration $t4b$, a direct transition from $t4g$ to $t4g^*$ is possible as shown in Fig. 8(a). The sequence involves a 30° rotation of the molecule around a single Si-C bond. This rotation can be induced, for example, by an STM tip that is either nonsymmetrical or is positioned off center with respect to the molecule. Similarly, a direct transition between $t4g$ and $t4e^*$ is also possible by means of a similar mechanism, see Fig. 8(b). In both cases the molecule arrives back at configuration $t4c$ performing in total the $3a_0$ translation, and the configuration $t4g$ acts as the bifurcation point. These manipulation pathways would become periodic if the same mechanism (pivoting over a single bond) is repeated several times. Otherwise, several pathways (of either $3a_0$ or $4a_0$ periodicities) may alternate resulting in some variation of the observed tip trajectories.

The $t4i \rightarrow t4i^* \rightarrow t4i \rightarrow \dots$ sequence suggested above to explain the observed tip traces with $2a_0$ periodicity, is based

on the pivoting mechanism over two C-Si bonds. This sequence may be unlikely as it is based on the least energetically favorable on-the-trough adsorption site. If we assume, however, that the molecule pivots over a single C-Si bond, then an alternative mechanism as shown in Fig. 8(c) can be suggested which is still based on the two most energetically favorable configurations. As in the cases of the $3a_0$ sequences, the proposed $2a_0$ trajectory can be induced by an STM tip that exerts an additional rotational momentum on the molecule around an axis perpendicular to the surface in addition to the translational motion.

The sequences discussed above may account for the experimentally observed trajectories with periodicities of $2a_0$ and $3a_0$. They also explain that the *periodicities* in observed tip trajectories may not be observable in every experiment as in order for them to happen it is required that the tip acts on the molecule at its center and in the direction of the trough with high accuracy. As was explained in Sec. II B, this is difficult to achieve and control in experiment, especially at room temperature.

The manipulation mechanisms considered so far correspond to the on-the-trough displacement of the molecule. We shall now consider *on-the-row* manipulation pathways for the completeness of this study. Analyzing possible transitions that can connect all eight known stable row sites upon pivoting over the front two C-Si bonds, we find that for most configurations, there is only one possible successor configuration along the manipulation path: $r2b \rightarrow r2g$; $r2c \rightarrow r2c^*$; $r2d \rightarrow r2c$; $r2e \rightarrow r2f$; $r2f \rightarrow r2a$; $r2g \rightarrow r2b$; $r2h \rightarrow r2a$; $r2h^* \rightarrow r2c$ and $r2f^* \rightarrow r2e$. There are only two geometries that allow two possibilities of transitions: (i) $r2a$ may go either to $r2h^*$ or $r2f^*$ and (ii) $r2c^* \rightarrow r2h$ or $r2d$.

Combining all these elementary pivoting steps into the rolling sequences, we arrive at the following four trajectories shown in Fig. 7(b). The lowest energy sequence $r2a \rightarrow r2f^* \rightarrow r2e \rightarrow r2f \rightarrow r2a \rightarrow \dots$ possesses the $4a_0$ periodicity. The sequence $r2b \rightarrow r2g \rightarrow r2b \rightarrow \dots$ has the $2a_0$ periodicity, while $r2a \rightarrow r2h^* \rightarrow r2c \rightarrow r2c^* \rightarrow r2h \rightarrow r2a \rightarrow \dots$ has the $5a_0$ periodicity. If the site $r2c^*$ is followed by the $r2d$ configuration, then the $3a_0$ periodic sequence may also be possible: $r2c \rightarrow r2c^* \rightarrow r2d \rightarrow r2c \rightarrow \dots$. The latter two sequences involve the highest-energy structures. Note that there are two groups of sequences with no possibilities of transitions between sites associated with them: first, the $2a_0$ periodic sequence based on configurations $r2b$ and $r2g$, and second, the three other sequences involving configurations $r2a$, $r2c$, $r2d$, $r2e$, $r2f$, and $r2h$. The $2a_0$ periodic sequence is determined uniquely by the initial adsorption configuration $r2b$ or $r2g$. In other cases the branching off at the $r2a$ or $r2c^*$ sites may result in a different sequence or alteration of sequences and thus broken periodicity. The C₆₀ manipulation path on the row is therefore likely to be more complex and have a less defined periodicity than the in-the-trough path.

Note that on-the-row manipulation has not yet been observed experimentally. The likely explanation for this is that the on-the-row configurations are less stable than those in the trough, and also attempts to manipulate a molecule adsorbed on the row are likely to lead it to be displaced into the trough. This is especially the case if the tip acts on the molecule not exactly in the direction along the row. As has been

discussed already, this is a very likely situation in the real experiment.

The energies of the adsorption configurations along the pathways considered above range between -2.6 and -0.8 eV. Note that we do not know the energy barriers for the molecule to overcome for most of the transitions between pairs of stable sites. However, from our *ab initio* calculations presented in Sec. III B for the first two elementary steps along the path $t4c \rightarrow t4g \rightarrow t4b \rightarrow t4g^* \rightarrow t4c \dots$, we infer that the barriers are likely to be of the order of 2 eV, and thus the molecule should be immobile at room temperature, so that it can only be displaced by an external force exerted, e.g., by an STM tip.

To summarize this section, a number of possible manipulation pathways for the C₆₀ molecule moving along the trough and row were considered and compared with experimentally recorded STM manipulation tip trajectories. We propose sequences of adsorption configurations that account for the experimentally observed tip trajectories along the trough including both periodic and aperiodic traces.

V. CONCLUSIONS

We reported on a large variety of constant current room temperature STM tip traces of the repulsive manipulations of the C₆₀ molecule in the trough on the Si(001) surface. Some of the traces demonstrate wave forms with clear periodicity of two, three, and four dimer-dimer distances a_0 and may extend for tens of Å. Some others show a more complex behavior with switching between different wave forms and/or systematic changes.

To explain the $4a_0$ periodic sequences, we have undertaken a series of *ab initio* density functional theory calculations, following the same method as in our preliminary work,⁴ in order to reexamine the first two elementary manipulation steps of the most energetically favorable in-the-trough path. In comparison with the earlier work,⁴ our present calculations include the BSSE correction and also we have used a number of different methods to force the molecule to move. In addition, in order to facilitate comparison with the room temperature STM experiments, the symmetrical $p(2 \times 1)$ Si(001) surface was considered as the reference system in calculating the binding energies along the path.

In agreement with the earlier study,⁴ the calculations show that the molecule moves between a series of stable adsorption configurations with four Si-C bonds to the surface via intermediate states with two Si-C bonds. Examination of bonding in the molecule and the surface reveals that the movement of the molecule proceeds via sequential breaking and formation of Si-C bonds to the surface according to a pivoting mechanism: immediately after the transition point, there are two bonds between the molecule and the surface, over which the molecule rolls. Energy barriers of ~ 2 eV are involved in such motion, they are caused by bond stretching and deformation of the molecule and the surface. Changes in the electron density distribution in the C₆₀-silicon system have also been systematically studied. They confirm the Si-C bond breaking and new bond formation and show that there are significant changes in the electron density distribu-

tion in the C_{60} molecule during manipulation (self-diffusion). Note that our calculated energy barriers are somewhat overestimated due to the constrained minimization technique used.

In order to understand the complex variety of observed manipulation traces, we have also analyzed all possible manipulation paths between stable adsorption sites both along the trough and the row. We find that a large number of different manipulation sequences are possible, although not all of them may be easily achieved due to likely high energy barriers and/or low binding energies of the stable structures involved. In particular, several $4a_0$ periodic sequences have been suggested that may account for the observed $4a_0$ periodic wave forms.

In order to explain the observed $3a_0$ periodic tip traces, we suggested an altered pivoting mechanism according to which the molecule pivots over one, rather than two, C-Si bonds, and a pair of possible detailed molecule trajectories corresponding to this mechanism have been proposed. The observed $2a_0$ periodic traces, reported here for the first time, have also been explained as resulting from either a special double-bond pivoting trajectory involving the configuration $t4i$ of the molecule in the trough, or a different mechanism that we consider more likely, in which the molecule pivots over a single C-Si bond, similarly to the $3a_0$ sequence. The observed aperiodic tip traces are explained by a nonsymmetric position of the tip with respect to the molecule or by a lack of precision in its manipulation direction, the factors which are difficult to avoid in real room temperature experiments, or both. These factors result in frequent switches be-

tween different manipulation sequences that appear as aperiodic tip trajectories in the experiment.

We believe, that the described simulations are also relevant for the self-diffusion of the C_{60} molecule on the Si(001) surface, indicating that the likely mechanism of the molecule diffusion is rolling, and this rolling can only happen at elevated temperatures due to rather high energy barriers.

Further studies on this system are currently under way, in particular, the effect of the STM tip on the manipulation mechanism is being investigated theoretically. This calculation will elucidate the role of the tip and will allow us to distinguish between tip-dependent and tip-independent processes. We firmly believe that the pivoting mechanism is the general mechanism whereby the molecule moves along the reactive Si surface, either in the absence or in the presence of the tip. Note that our theoretical results on the C_{60} manipulation are also of relevance to a possible AFM assisted manipulation in which controlled translation is driven by the force between tip and molecule.

ACKNOWLEDGMENTS

We would like to acknowledge the computer time on the HPCx supercomputer via the Materials Chemistry Consortium. N.M. and C.H. would like to acknowledge the financial support from the NANOMAN (NMP-CT-2003-505660) project and EPSRC (Grant No. GR/R97023/01), respectively.

-
- ¹D. Eigler and E. Schweizer, *Nature (London)* **344**, 524 (1990).
²L. Bartels, G. Meyer, and K. H. Rieder, *Phys. Rev. Lett.* **79**, 697 (1997).
³P. Beton, A. Dunn, and P. Moriarty, *Appl. Phys. Lett.* **67**, 1075 (1995).
⁴D. L. Keeling, M. J. Humphry, R. H. J. Fawcett, P. H. Beton, C. Hobbs, and L. Kantorovich, *Phys. Rev. Lett.* **94**, 146104 (2005).
⁵P. Moriarty, Y. R. Ma, M. D. Upward, and P. H. Beton, *Surf. Sci.* **407**, 27 (1998).
⁶L. Pizzagalli and A. Baratoff, *Phys. Rev. B* **68**, 115427 (2003).
⁷E. Kaxiras, *Thin Solid Films* **272**, 386 (1996).
⁸F. Rosei, M. Schunack, Y. Naitoh, P. Jiang, A. Gourdon, E. Laegsgaard, I. Stensgaard, C. Joachim, and F. Besenbacher, *Prog. Surf. Sci.* **71**, 95 (2003).
⁹N. Lorente and H. Ueba, *Eur. Phys. J. D* **35**, 341 (2005).
¹⁰P. D. Godwin, S. D. Kenny, and R. Smith, *Surf. Sci.* **529**, 237 (2003).
¹¹C. Hobbs and L. Kantorovich, *Nanotechnology* **15**, S1 (2004).
¹²C. Hobbs, L. Kantorovich, and J. Gale, *Surf. Sci.* **591**, 45 (2005).
¹³X.-D. Wang, T. Hashizume, H. Shinohara, Y. Saito, Y. Nishina, and T. Sakurai, *Phys. Rev. B* **47**, 15923 (1993).
¹⁴R. M. Tromp, R. J. Hamers, and J. E. Demuth, *Phys. Rev. Lett.* **55**, 1303 (1985).
¹⁵D. Chen and D. Sarid, *Surf. Sci.* **329**, 206 (1995).
¹⁶D. L. Keeling, M. J. Humphry, P. Moriarty, and P. H. Beton, *Chem. Phys. Lett.* **366**, 300 (2002).
¹⁷M. J. Humphry, R. Chettle, P. Moriarty, M. D. Upward, and P. H. Beton, *Rev. Sci. Instrum.* **71**, 1698 (2000).
¹⁸J. M. Soler, E. Artacho, J. D. Gale, A. García, J. Junquera, P. Ordejón, and D. Sánchez-Portal, *J. Phys.: Condens. Matter* **14**, 2745 (2002).
¹⁹J. P. Perdew, K. Burke, and M. Ernzerhof, *Phys. Rev. Lett.* **77**, 3865 (1996).
²⁰S. Boys and F. Bernardi, *Mol. Phys.* **19**, 553 (1970).
²¹T. Uda, H. Shigekawa, Y. Sugawara, S. Mizuno, H. Tochiara, Y. Yamashita, J. Yoshinobu, K. Nakatsuji, H. Kawai, and F. Komori, *Prog. Surf. Sci.* **76**, 147 (2004).
²²J. Yoshinobu, *Prog. Surf. Sci.* **77**, 37 (2004).
²³L. Kantorovich and C. Hobbs, *Phys. Rev. B* **73**, 245420 (2006).
²⁴T. Xiao and K. Liao, *Nanotechnology* **14**, 1197 (2003).
²⁵Z. Zhang, Z. Pan, Y. Wang, Z. Li, and Q. Wei, *Mod. Phys. Lett. B* **17**, 877 (2003).
²⁶M. Moalem, M. Balooch, A. Hamza, and R. Ruoff, *J. Phys. Chem.* **99**, 16736 (1995).
²⁷H. Jonsson, G. Mills, and K. W. Jacobsen, *Classical and Quantum Dynamics in Condensed Phase Simulations* (World Scientific, New York, 1998), chap. Nudged Elastic Band Method for Finding Minimum Energy Paths of Transitions.
²⁸G. Mills, H. Jonsson, and G. K. Schenter, *Surf. Sci.* **324**, 305 (1995).